A Combined Density Functional and Molecular Dynamics Study on Ethylene Insertion into the $Cp_2ZrEt-MeB(C_6F_5)_3$ Ion-Pair

Mary S. W. Chan and Tom Ziegler*

Department of Chemistry, University of Calgary, Calgary, Alberta, Canada T2N 1N4

Received June 9, 2000

Several aspects related to the insertion process of an ethylene molecule into the Zr−ethyl (Et) bond of the $Cp_2ZrEt-MeB(C_6F_5)_3$ contact ion-pair were examined by static density functional and first-principles molecular dynamic methods. The most stable conformer of this contact ion-pair can be described as having the anion coordinated to the Zr on the backside of the ethyl chain via a methyl bridge. This most stable conformation of $Cp_2ZrEt-MeB(C_6F_5)_3$ contained no agostic interactions with any of the hydrogen atoms on the ethyl chain. The insertion pathway studied considers the ethylene to approach the metal center of the contact ion-pair from the side opposite the anion. The ethyl chain rotates away from the olefin and the anion was pushed out of the coordination sphere of the zirconium before complexation occurs. The insertion occurs rapidly and apparently without significant barrier after successful complexation of the olefin. The behavior of the counterion after insertion was also examined. Considerations were given to an associative mechanism in which the counterion recombines with the catalyst to form a new contact ion-pair. Also considered was a dissociative mechanism in which the counterion continues to detach from the cation via the formation of an olefin-separated ion-pair. Either mechanism is a possibility depending on the conditions under which the polymerization is carried out.

I. Introduction

Despite recent investigations into the development of single-site olefin polymerization catalysts that do not contain cyclopentadienyl ligands, group IV metallocenes remain one of the most active commercially viable catalysts.[1] The metallocenes and their related organometallic complexes have already been the subject of intense experimental[2] and theoretical[3] studies. A generally accepted polymerization mechanism for these catalysts has been established,[4] and the three fundamental processes of activation, insertion, and termination are depicted in Scheme 1. The metallocene complexes need to be activated by a Lewis acid such as trispentafluorophenylborane [$B(C_6F_5)_3$] to form an electron-deficient metal center that acts as the true polymerization catalyst. Previous studies have shown that the reaction of dialkylmetallocenes with $B(C_6F_5)_3$ results in the formation of a contact ion-pair (labeled as structure **1** in Scheme 1).[5] Up until very recently, it was believed that these ion-pairs completely dissociate into their ionic components, producing a cation with a coordinately unsaturated metal center to which a molecule of the monomer can bind. The growth of the polymer chain occurs from this point by the insertion of the monomer into the metal carbon bond of the already existing chain, as depicted by the insertion reactions in Scheme 1. Several mechanisms for termination of the polymer chain have been considered in theoretical studies. The lowest energy pathway depicted in Scheme 1 occurs by the transfer of a β-hydrogen on the polymer chain to a monomer molecule.[3,4]

There has been numerous experimental evidence to suggest that the counterion in some cases might play a critical role in the polymerization process by controlling ion-pair formation and dissociation equilibria.[2d,6] However, earlier theoretical studies have concentrated on the cationic metal reaction center in order to reduce the size of the molecular system down to manageable calculations. It is only within the past few years that

(1) (a) Stephan, D. W.; Guérin, F.; Spence, R. E. v. H.; Koch, L.; Gao, X.; Brown, S. J.; Swabey, J. W.; Wang, Q.; Xu, W.; Zoricak, P.; Harrison, D. G. *Organometallics* **1999**, *18*, 2046. (b) Britovsek, G. J. P.; Gibson, V. C.; Wass, D. F. *Angew. Chem., Int. Ed. Engl.* **1999**, *38*, 428.

(2) (a) Ewart, S. W.; Sarsfield, M. J.; Williams, E. F.; Baird, M. C. *J. Organomet. Chem.* **1999**, *579*, 106. (b) Harlan, C. J.; Bridgewater, B. M.; Hascall, T.; Norton, J. R. *Organometallics 18*, 3827. (c) Beswick, C. L.; Marks, T. J. *Organometallics* **1999**, *18*, 2410. (d) Dahlmann, M.; Erker, G.; Nissinen, M.; Fröhlich, R. *J. Am. Chem. Soc.* **1999**, *121*, 2820. (e) Deck, P. A.; Beswick, C. L.; Marks, T. J. *J. Am. Chem. Soc.* **1998**, *120*, 1772. (f) Bochmann, M. *J. Chem. Soc., Dalton Trans.* **1996**, 255.

(3) (a) Klesing, A.; Bettonville, S. *Phys. Chem. Chem. Phys.* **1999**, *1*, 2373. (b) Froese, R. D. J.; Musaev, D. G.; Morokuma, K. *Organometallics* **1999**, *18*, 373. (c) Margl, P. M.; Woo T. K.; Ziegler, T. *Organometallics* **1998**, *17*, 4997. (d) Lohrenz, J. C. W.; Woo, T. K.; Ziegler, T. *J. Am. Chem. Soc.* **1995**, *117*, 12793.

(4) Thorshaug, K.; Støvneng, J. A.; Rytter, E.; Ystenes, M.; *Macromolecules* **1998**, *31*, 7149.

(5) (a) Chen, Y.-X.; Marks, T. J. *Organometallics* **1997**, *16*, 3649. (b) Wang, Q.; Quyoum, R.; Gillis, D. J.; Jeremic, D.; Tudoret, M.-J.; Baird, M. C. *J. Organomet. Chem.* **1997**, *527*, 7. (c) Yang, X.; Stern, C. L.; Marks, T. J. *J. Am. Chem. Soc.* **1994**, *116*, 10015.

(6) (a) Luo, L.; Marks, T. J. *Top. Catal.* **1999**, *7*, 97. (b) Chen, Y.-X.; Metz, M. V.; Li, L.; Stern, C. L.; Marks, T. J. *J. Am. Chem. Soc.* **1998**, *120*, 6287. (c) Small, B. L.; Brookhart, M.; Bennett, A. M. A. *J. Am. Chem. Soc.* **1998**, *120*, 4049. (d) Jia, L.; Yang, X.; Stern, C. L.; Marks, T. J. *Organometallics* **1997**, *16*, 842. (e) Brintzinger, H. H.; Fischer, D.; Mülhaupt, R.; Rieger, B.; Waymouth, R. M. *Angew. Chem., Int. Ed. Engl.* **1995**, *34*, 1143.

10.1021/om000486s CCC: $19.00
Publication on Web 11/02/2000

Scheme 1. Fundamental Steps of the Polymerization Process for Metallocenes

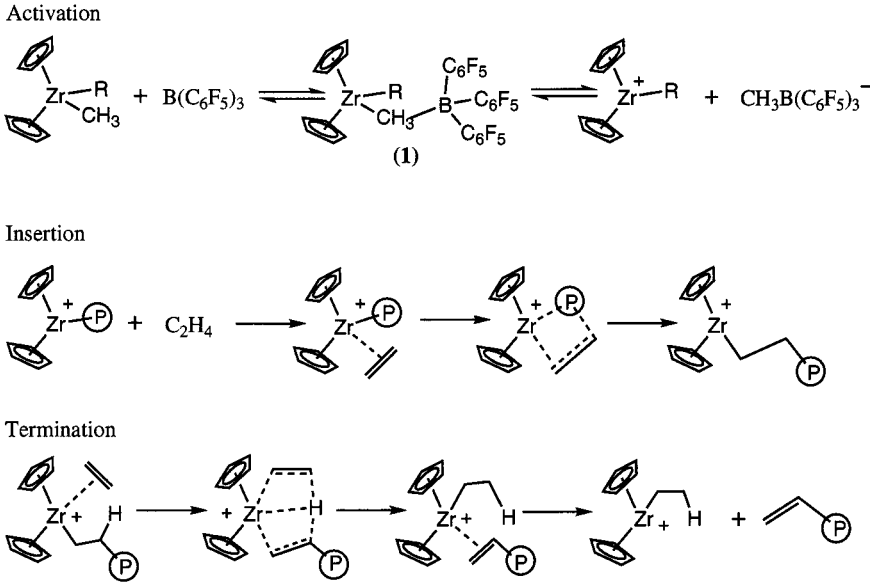

advances in computer technology made the study of these catalysts including the counterion a possibility. So far, the theoretical studies have focused only on the activation step of the polymerization process.[3a,7] The few exceptions have been the insertion of olefins into the $H_2Si(C_5H_4)(^tBuN)TiMe-MeB(C_6F_5)_3$ ion-pair by Lanza,[8] the $Cp_2(Ti/Zr)Me-Cl_2Al[O(AlMe_3AlHMe]_2$ ion-pair by Fusco,[9] and the $Cl_2TiMe(\mu\text{-}Cl)_2AlH_2$ ion-pair by Bernardi.[10] These studies have suggested that the reaction potential surface for insertion into the ion-pairs are significantly different from those obtained previously by considering the cationic fragment alone. To further study the role of the counterion in the polymerization process, the focus of the present study is an in-depth investigation of the ethylene insertion into the $Cp_2ZrEt-MeB(C_6F_5)_3$ ion-pair using a combination of density functional and first-principles molecular dynamics methods.[11] Our study differs from the previous investigation by Lanza[8] et al. in that we represent the growing chain by an ethyl rather than a methyl group. Also our calculations will concentrate on the zirconium-based $CpZrEt^+$ system rather than the titanium-based constraint geometry catalyst $H_2Si(C_5H_4)(^tBuN)TiMe^+$.

II. Computational Details

Stationary points on the potential energy surface were calculated with the Amsterdam Density Functional (ADF) program (version 2.3.3) developed by Baerends et al.[12] and vectorized by Ravenek.[13] The numerical integration scheme applied for the calculations were developed by te Velde et al.[14] The geometry optimization procedure was based on the method from Versluis and Ziegler.[15] Energy differences were calculated by augmenting the local exchange−correlation potential by Vosko et al. with Perdew and Wang's nonlocal correlation and exchange corrections.[16] The electronic configuration of zirconium was treat with a Slater type triple-ζ basis function for the 5s, 4p, and 4d shells, a double-ζ basis for 4s, and a single-ζ 5p polarization function. The $[Ar]3d^{10}$ core on zirconium was treated with the frozen core approximation. For the second-row elements B, C, and F, the $1s^2$ electronic configuration was treated with the frozen core approximation, and a double-ζ basis was used for the 2s and 2p shells augmented with a single-ζ 3d polarization function. The hydrogen atom was represented by a double-ζ basis function for the 1s orbital and a single-ζ 2p polarization function. The polarization functions were omitted for the carbon and hydrogen atoms on the cyclopentadienyl rings. A set of auxiliary s, p, d, f, and g STO functions centered on all nuclei was used to fit the molecular density and represent Coulomb and exchange potentials accurately in each SCF cycle.[17] In view of the fact that all systems investigated in this work show a large HOMO−LUMO gap, a spin-restricted formalism was used for all calculations. The transition state geometries and energies were obtained by a series of geometry optimization along a fixed reaction coordinate, while all other parameters were optimized. The transition state was taken to be at geometry where the gradient on the reaction coordinate was less than the threshold set for the optimization procedure. The reaction coordinate used for the insertion reaction was the distance between the α carbon and one carbon atom of the approaching ethylene (i.e., the C−C bond that is being formed). Solvation energies for toluene ($\epsilon = 2.38$) were evaluated based on optimized gas-phase structures calculated by the conductor-like screening model (COSMO) available within the ADF program.[18]

All reported molecular dynamics simulations were carried out with the Car−Parrinello projector augmented wave (CP-PAW) method developed by Blöchl.[19] The wave function was expanded in plane waves up to an energy cutoff of 30 Ry. The

(7) Chan, M. S. W.; Vanka, K.; Pye, C. C.; Ziegler, T. *Organometallics* **1999**, *18*, 4624. (b) Zuccaccia, C.; Macchioni, A.; Orabona, I.; Ruffo, F. *Organometallics* **1999**, *18*, 4367.

(8) (a) Lanza, G.; Fragalà, I. L.; Marks, T. J. *J. Am. Chem. Soc.* **1998**, *120*, 8257. (b) Lanza, G.; Fragalà, I. L. *Top. Catal.* **1999**, *7*, 45.

(9) Fusco, R.; Longo, L.; Proto, A.; Masi, F.; Garbassi, F. *Macromol. Rapid Commun.* **1998**, *19*, 257.

(10) Bernardi, F.; Bottoni, A.; Miscione, G. P. *Organometallics* **1998**, *17*, 16.

(11) (a) Woo, T. K.; Blöchl, P. E.; Ziegler, T. *J. Phys. Chem. A* **2000**, *104*, 121. (b) Margl, P. M.; Lohrenz, J. C. W.; Ziegler, T.; Blöchl, P. *J. Am. Chem. Soc.* **1996**, *118*, 4434.

(12) (a) Baerends, E. J.; Ellis, D. E.; Ros, P. *Chem. Phys.* **1973**, *2*, 41. (b) Baerends, E. J.; Pos, P. *Chem. Phys.* **1973**, *2*, 52.

(13) Ravenek, W. In *Algorithms and Applications on Vector and Parallel Computers*; te Riele, H. J. J., Dekker, T. J., van de Horst, H. A., Eds.; Elsevier: Amsterdam, The Netherlands, 1987.

(14) te Velde, G.; Baerends, E. J. *J. Comput. Chem.* **1992**, *99*, 84.

(15) Versluis, L.; Ziegler, T. *J. Chem. Phys.* **1988**, *88*, 322.

(16) (a) Vosko, S. H.; Wilk, L.; Nusair, M. *Can. J. Phys.* **1980**, *58*, 1200. (b) Perdew, J. P. *Phys. Rev. B* **1992**, *46*, 6671.

(17) Krijn, J.; Baerends, E. J. *Fit Functions in the HFS-Method*; Free University of Amsterdam, 1984.

(18) Pye, C. C.; Ziegler, T. *Theor. Chim. Acta* **1999**, *101*, 396.

(19) Blöchl, P. E. *Phys. Rev. B* **1994**, *50*, 17953.

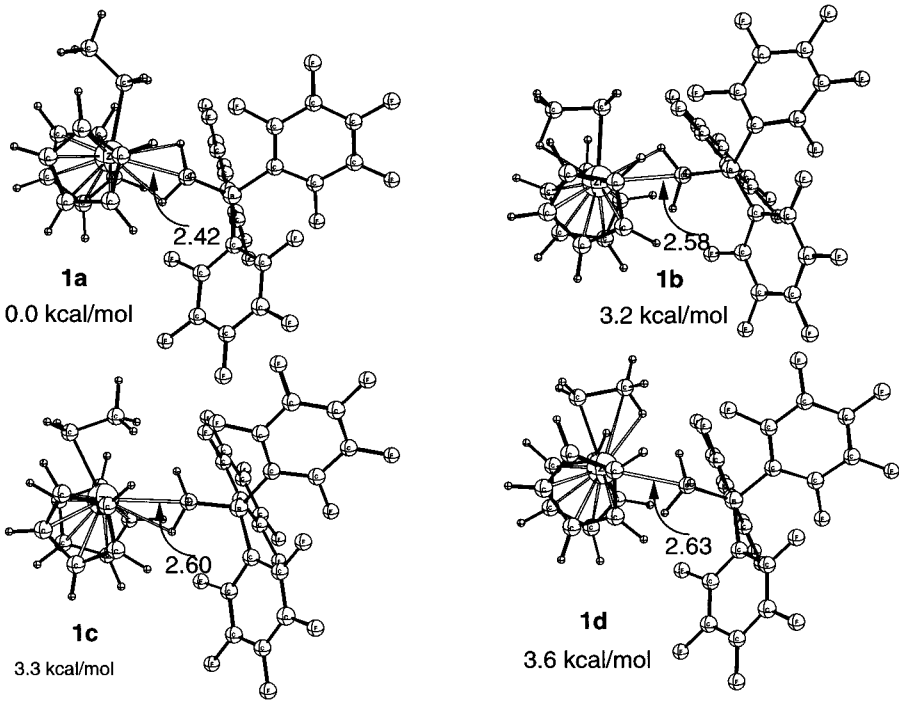

Figure 1. Structures of the contact ion-pair: $Cp_2ZrEt-MeB(C_6F_5)_3$.

frozen-core approximation was applied for shells below the 4d electrons of Zr and for the 1s electrons of the second-row elements B, C, and F. Core data were imported from scalar relativistic atomic calculations. All simulations were performed using the local density approximation in the parametrization of Perdew and Zunger, with gradient corrections due to Becke and Perdew.[20] Periodic boundary conditions were used with a 19.8 Å fcc unit cell. A charge isolation scheme developed by Blöchl was also used to prevent electrostatic interactions between neighboring unit cells.[21] To achieve an evenly distributed thermal excitation, the nuclei were brought to a temperature of 300 K by applying a sequence of 30 sinusoidal pulses; their excitation vectors were chosen to be orthogonal to the already excited modes. A temperature of 300 K was maintained for all simulations by a Nosé thermostat, which creates a canonical (NVT) ensemble.[22] The fictitious kinetic energy of the electrons was controlled in a similar fashion by a Nosé thermostat.[23] The true masses of the nuclei were rescaled to 5.0 for Zr, 2.0 for B, C, and F, and 1.5 for H in order to span large portions of configuration space in minimum time. A time step of 4.7 au (~0.11 fs) was used to integrate the equations of motion. To sample phase space in the vicinity of the transition state, a reaction coordinate (RC) was chosen to be kept constrained during the dynamics using SHAKE constraints.[24] All other degrees of freedom are allowed to evolve naturally in time. By slowly changing the value of the constraint, phase space in the vicinity of the transition state can be sampled dynamically, leading to undisturbed dynamics for all motions that are orthogonal to the RC and to fictitious dynamics along the RC. This "slow-growth" technique allows us to investigate even high-lying transition states.[11] The total scan time was about 28 000 time steps, which required the use of six DEC Alpha machines for 3 months. The number of time steps were sufficient to acquire a qualitative picture of the insertion process, but insufficient to determine the free energy potential curve along the reaction path.

III. Results and Discussion

a. Determination of the Resting State. The length of the alkyl chain required to accurately model the growing polymer chain has been previously examined.[25] Studies on the methyl, ethyl, propyl, and pentyl chains have been conducted on the unassociated zirconocene cations to determine the lowest energy conformer. These studies found that a β-agostic structure was the most stable conformer for alkyl chains longer than methyl and concluded that this type of structure constitutes the resting state between two insertions. Therefore, a minimum of an ethyl chain is needed to accurately represent the behavior of a growing polymer chain. On the basis of these results, the ethyl chain was chosen and four conformers of the $Cp_2ZrEt-MeB(C_6F_5)_3$ ion-pair were examined by ADF calculations. The optimized structures of these contact ion-pairs along with selected interatomic distances in angstroms are shown in Figure 1. In structures **1a** and **1b**, the anion is coordinated to the metal from the backside of the ethyl chain. Both of these conformers are lower in energy than structures **1c** and **1d**, where the anion is located on the frontside. This is consistent with the previously examined reactions of zirconocene cations with substituted phosphine bases, where it was found that they preferentially coordinate to the backside.[26] In contrast with previous studies, the conformers without β-agostic interactions were found to be more stable. For the backside conformers, the one without the β-agostic interaction, **1a**, is

(20) (a) Perdew, J. P.; Zunger, A. *Phys. Rev. B* **1981**, *23*, 5048. (b) Becke, A. D. *Phys. Rev.* **1988**, *A38*, 3098. (c) Perdew, J. P. *Phys. Rev. B* **1986**, *33*, 8822. (d) Perdew, J. P. *Phys. Rev. B* **1986**, *34*, 7406.
(21) Blöchl, P. E. *J. Chem. Phys.* **1995**, *103*, 7422.
(22) (a) Hoover, W. G. *Phys. Rev. A* **1985**, *31*, 1695. (b) Nosé, S. *Mol. Phys.* **1984**, *52*, 255.
(23) Blöchl, P. E.; Parrinello, M. *Phys. Rev. B* **1992**, *45*, 9413.
(24) Ryckaert, J.-P.; Ciccotti, G.; Berendsen, H. J. C. *J. Comput. Phys.* **1977**, *23*, 327.
(25) (a) Lohrenz, J. C. W.; Woo, T. K.; Fan, L.; Ziegler, T. *J. Organomet. Chem.* **1995**, *497*, 91. (b) Woo, T. K.; Fan, L.; Ziegler, T. *Organometallics* **1994**, *13*, 2252. (c) Woo, T. K.; Fan, L.; Ziegler, T. *Organometallics* **1994**, *13*, 423.
(26) Alelyunas, Y. W.; Baenziger, N. C.; Bradley, P. K.; Jordan, R. F. *Organometallics* **1994**, *13*, 148.

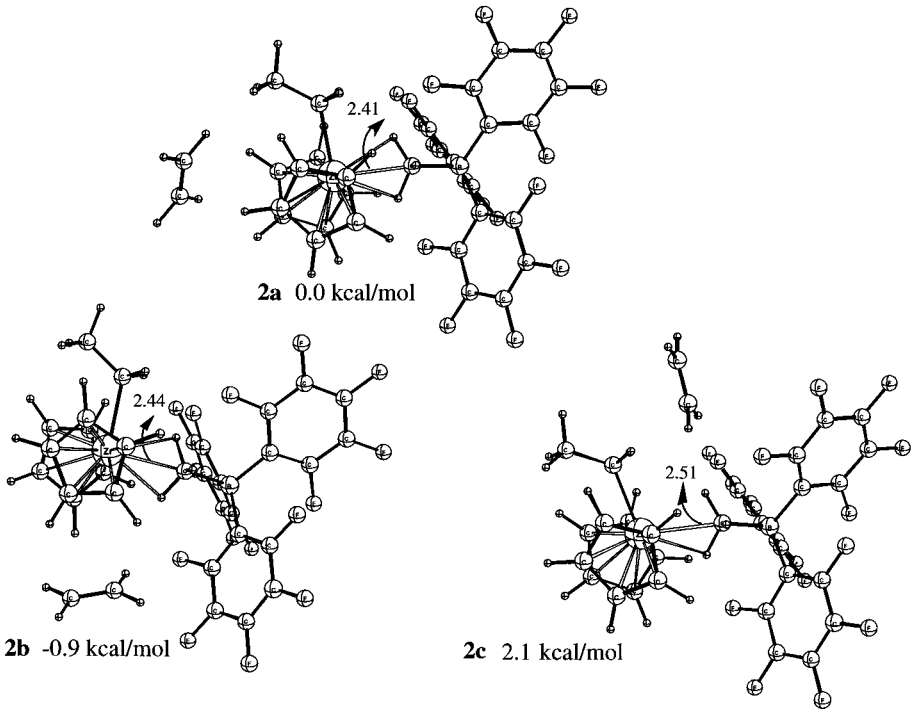

Figure 2. Structures and relative energies of complexes for possible approaches of the olefin to the ion-pair.

more stable than the one with the β-agostic interaction, **1b**, by 3.2 kcal/mol. The energy difference is not as pronounced for the frontside conformers. However, the one without the β-agostic interaction, **1c**, is still more stable by 0.3 kcal/mol. This observation adds to the growing pool of evidence that including the anion in the coordination sphere of the metal can alter the behavior of the complex. The preference of these contact ion-pairs for conformers without β-agostic interactions can be rationalized by electronic and steric factors. The electron deficiency of the zirconium is already partly alleviated by coordination with the anion, making stabilization by agostic interactions less important than in the free cation. In addition, steric factors can also contribute to the relative instability of the β-agostic interaction in the ion-pairs. First, the ethyl chain is forced into a sterically unfavorable eclipsed position in the ion-pairs with a β-agostic interaction. Furthermore, the ethyl chain in these ion-pairs is also pulled toward the metal, causing more steric crowding.

b. Approach of the Ethylene. Insertion studies were initiated from the most stable conformer of the $Cp_2ZrEt-MeB(C_6F_5)_3$ contact ion-pair, **1a**. The insertion process is initiated by the advancement of the ethylene molecule toward the metal center. The three structures shown in Figure 2 represent the beginning of three different pathways to achieve ethylene coordination with the zirconium. The ethylene can approach the ion-pair opposite the anion, as indicated by the complex labeled **2a**, or opposite the ethyl chain, as indicated by complex **2b**. The final approach is for the ethylene to advance from between the polymer chain and the anion, as depicted by complex **2c**. The last pathway mentioned can be easily eliminated by virtue of the large steric repulsion between the ethylene molecule and aryl groups on the anion. This is reflected in the relative instability of complex **2c**. The slightly lower energy of complex **2b** compared to **2a** may suggest that olefin coordination is easier from the pathway where the ethylene approaches from the opposite side of the growing polymer chain. However, subsequent insertion from such a π-complex may be difficult due to the presence of the anion between the olefin and ethyl group, the two moieties that need to be in close proximity in order to form the new carbon−carbon bond. Therefore, the pathway initiated by complex **2a** was considered for further insertion studies. This choice of the reaction pathway is the same as the most energetically favorable pathway found from previous studies on the $H_2Si(C_5H_4)(^tBuN)TiMe-MeB(C_6F_5)_3$ ion-pair.[8]

c. Insertion. The insertion of one molecule of ethylene into the $Cp_2ZrEt-MeB(C_6F_5)_3$ ion-pair was studied using both static DFT calculations (ADF) and the DFT-based dynamic CP-PAW method.[19]

1. Dynamic Calculations. For the dynamic calculations, the starting structure was taken to be the complex **2a**, where the ethylene molecule is located on the opposite side of the anion. There is virtually no interaction between the olefin and the zirconium at this point, as indicated by the long distance of 4.17 Å between the midpoint of the olefin and the metal, which was taken as the reaction cordinate. The reaction was monitored from a distance of 4.17−2.30 Å. Important snapshots of the molecular geometries along the reaction coordinate are shown in Figures 3 and 4. The key interatomic distances are reported in angstroms. Structure **S1** shows the geometry of the ethylene and the contact ion-pair at the beginning of the simulation. The midpoint of the ethylene molecule is located 4.17 Å from the zirconium, far enough that there should be no substantial interaction between the two molecules at this point. The β carbon of the chain is pointed toward the olefin with a dihedral angle $C_\beta-C_\alpha-Zr-C_{(olefin)}$ of 11.4°. The first most noticeable geometrical change that occurs as the ethylene molecule approaches the zirconium is the rotation of the ethyl chain toward the anion in order to avoid repulsive steric interactions with the incoming olefin. The $C_\beta-C_\alpha-Zr-C_{(olefin)}$ dihedral angle

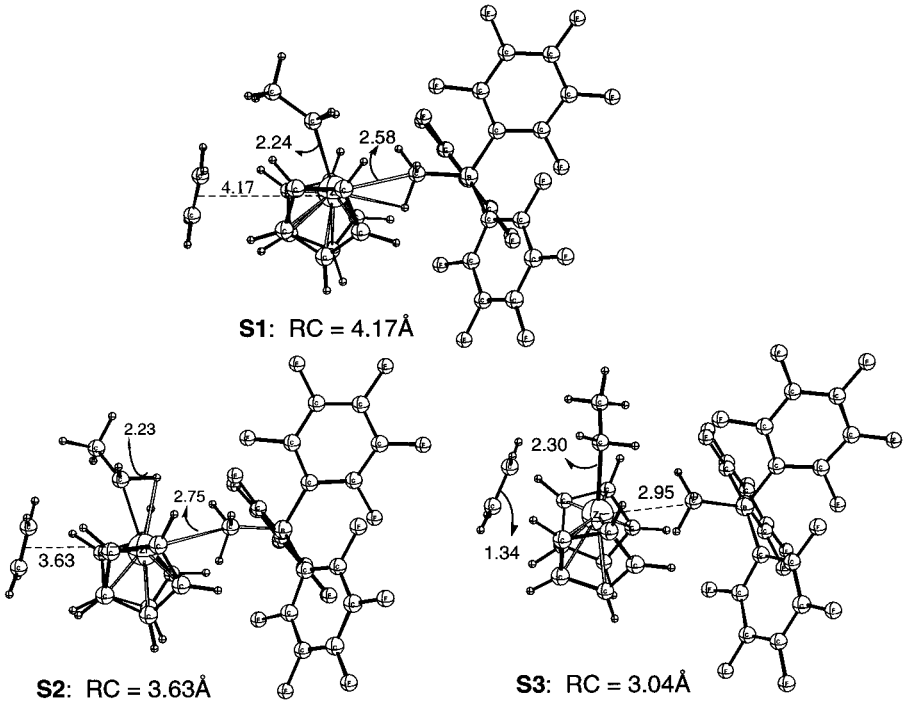

Figure 3. Selected structures along the reaction coordinate before olefin complexation obtained from the CP-PAW simulation.

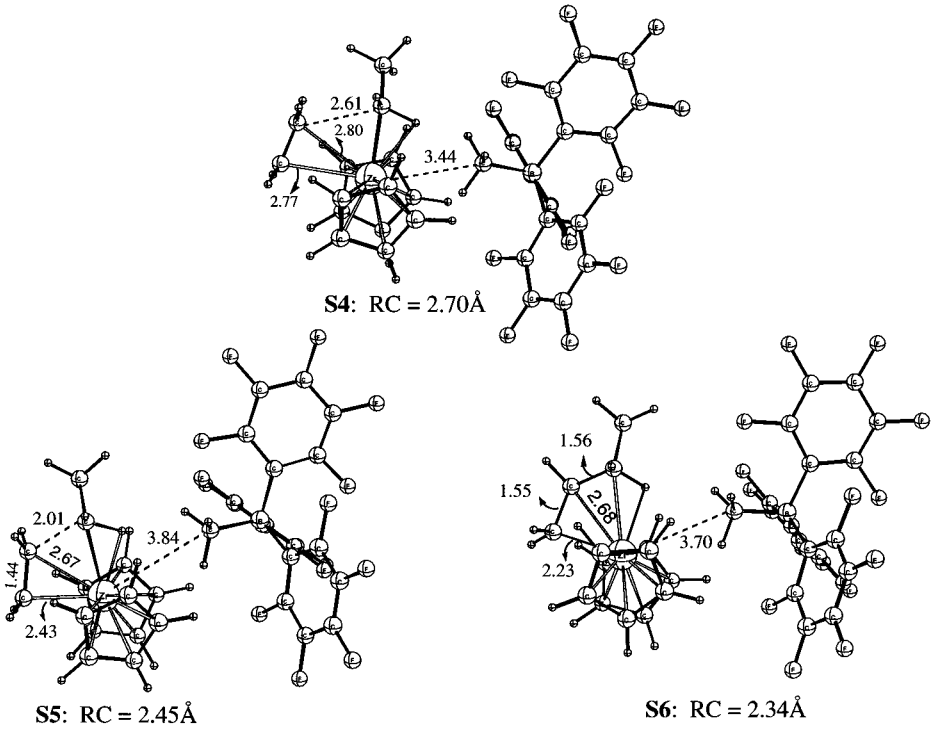

Figure 4. Selected structures along the reaction coordinate after olefin complexation obtained from the CP-PAW simulation.

increased to 71.0° in structure **S2**, which is taken after 7850 time steps. As the chain rotates, an α-agostic interaction develops between one of the hydrogen atoms on the α carbon and the metal. The second most noticeable change is that the anion is slowly being dissociated from the metal center, as indicated by the lengthening of the $C_{(methyl)}$−Zr distance from 2.58 Å at the beginning of the simulation to 2.75 Å in structure **S2**. The anion has moved far enough away that the agostic interaction between the zirconium and the hydrogen atoms in the methyl groups has been broken. The $MeB(C_6F_5)_3^-$ anion continues to move away from the zirconium and completely leaves the coordination sphere, as illustrated by structure **S3**. The $C_{(methyl)}$−Zr distance has increased to 2.95 Å, and a lengthening of the C_α−Zr distance from 2.24 to 2.30 Å is also observed. The midpoint of the olefin is at 3.04 Å from the Zr, indicating that olefin complexation has not yet occurred. It should be noted that in structure **S3** the zirconium does not appear to be coordinated to either the anion or the ethylene, suggesting that the anion dissociates before complexation of the olefin can occur. Structure

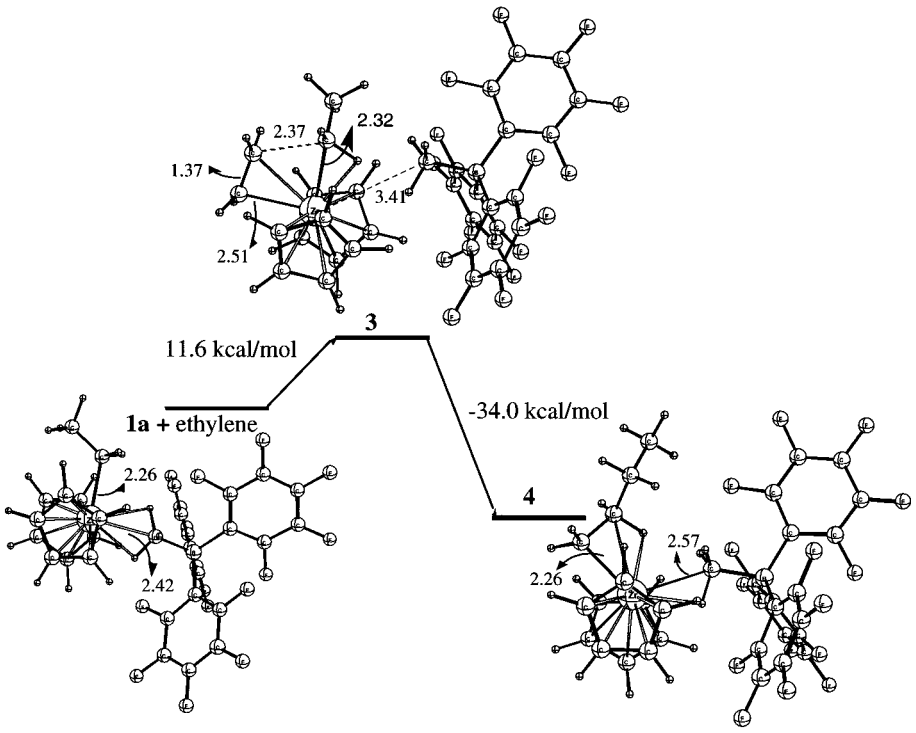

Figure 5. Insertion reaction energy profile obtained from ADF calculations.

S4, which resembles the structure of a olefin π-complex, was obtained after 21 450 time steps. The ethylene is almost symmetrically coordinated with the carbon atoms at 2.80 and 2.77 Å from the zirconium. There is a slight deviation from planarity in the ethylene molecule, as indicated by the improper torsion of 166.7° at one of the olefinic carbon atoms, but no significant lengthening of the C−C double bond is observed as yet. The $C_{(methyl)}-Zr$ distance is now at 3.44 Å, indicating continued displacement of the anion moiety upon complexation. The most active region of the molecule after successful complexation of the ethylene molecule is the movement of this moiety toward the α carbon in preparation for insertion. This is evidenced by dramatic shortening of the $C_{(olefin)}-C_{(\alpha)}$ bond from 2.61 Å in structure **S4** to 2.01 Å in structure **S5** and the lengthening of the $Ni-C_{(\alpha)}$ bond from 2.26 to 2.36 Å within the same structures. Geometrical changes within the ethylene also point to insertion with the lengthening of the C−C double bond from 1.36 to 1.44 Å that is accompanied by the shortening of one $C_{(olefin)}-Zr$ bond from 2.77 to 2.43 Å. Further deviation from planarity is indicated by the decrease of the improper torsion to 138.7°. Finally, the kinetic product of the insertion with the γ-agostic butyl chain is observed in structure **S6**. The formation of the new carbon−metal bond is complete at 2.23 Å. The C−C double bond has been broken, as indicated by the long bond distance of 1.55 Å and the formation of the new C−C bond occurring at a bond length of 1.56 Å. The number of time steps used in the simulation was sufficient to study the qualitative features of the insertion reactions. However, they were not sufficient to calculate enthalpies and free energies. An estimate of these quantities would have required 3−4 times the computational effort. We shall instead determine the energetics of the insertion process from static DFT calculations.

2. Static Calculations. Static calculations using the ADF program were performed to obtain better energies for the insertion reaction. The transition state for the insertion was located as described in the Computational Details section. The reaction profile for the insertion is shown in Figure 5. The reference energy is taken as the sum of the ion-pair **1a** and an ethylene molecule. In this ion-pair, the $C_{(methyl)}-Zr$ distance is 2.42 Å, close enough to facilitate agostic interactions from two of the hydrogen atoms connected to the methyl carbon. The cyclopentadienyl ligands adopt a staggered conformation to minimize steric interactions. The transition state (labeled as structure **3**) lies 11.6 kcal/mol above the ion-pair **1a** and ethylene molecule. This can be compared with the 11.1 kcal/mol insertion barrier for propene estimated from dynamic NMR studies on the zirconocene−borate−betaine systems,[27] which must be considered as an upper bound for ethylene insertion. In the transition state, the anion has been replaced with the ethylene in the zirconium's coordination sphere. The $C_{(methyl)}-Zr$ distance has lengthened to 3.41 Å, disrupting any direct interaction of the methyl group with the metal center. The two carbon atoms of the ethylene are asymmetrically coordinate at 2.44 and 2.51 Å, indicating the formation of the new carbon metal bond. The β carbon of the ethyl chain has rotated toward the anion so that the olefin can approach the α carbon to form the new carbon−carbon bond. This bond length is at 2.37 Å in the transition state. The cyclopentadienyl ligands have adopted an eclipsed conformation in order to accommodate the olefin, and the metal center is now stabilized by an α-agostic interaction, as can be seen in structure **3** in Figure 5. This structure of the insertion transition state is similar to structure **S5** in Figure 4 obtained from the CP-PAW simulation. The product

(27) Karl, J.; Dahlman, M.; Erker, G. Bergander, K. *J. Am. Chem. Soc.* **1998**, *120*, 5643.

after insertion is a contact ion-pair with a butyl chain, as depicted by structure **4**. It lies 34.0 kcal/mol below the transition state or 22.4 kcal/mol below the ethyl ion-pair and a molecule of ethylene. The structure of this product is similar to the ion-pair **1a** in that the anion has been reattached to the zirconium with a $C_{(methyl)}$−Zr distance of 2.57 Å, and the cyclopentadienyl ligands have returned to the staggered conformation. The conformation of the butyl chain shows a β-agostic interaction. The structure of this β-agostic insertion product was obtained by geometry optimization starting from the transition state by relaxing the constraint on the C−C bond. This suggests the feasibility of recombining the ionic fragments to reproduce the contact ion-pair after each insertion in the gas phase.

The reaction pathway and the barrier to the insertion of an ethylene molecule into the Cp_2ZrEt−$MeB(C_6F_5)_3$ ion-pair have been determined by combining the strengths of the CP-PAW dynamic and static DFT computational methods used. The ethylene approaches the metal center from the opposite side of the where the anion is coordinated. As the olefin advances toward the zirconium, the ethyl chain used to model the growing polymer rotates away from the ethylene in order to minimize steric repulsions. At the same time, the anion is slowly being displaced from the coordination sphere. The first sign of olefin metal interaction occurs when the distance between the methyl group on the anion and the zirconium is at 3.32 Å, suggesting that the anion has been displaced before olefin complexation occurs. After successful complexation of the olefin, the system proceeds rapidly through an insertion transition state to produce the kinetic product with the γ-agostic butyl chain. Although the conditions of the present simulation prevent the observation of such behavior, previous simulations have suggested that such kinetic products rearrange to the thermodynamic products without any significant barriers.[28] The barrier to insertion was found to be 11.6 kcal/mol by density functional calculations, in good agreement with experimental estimates.

d. Formation of Olefin-Separated Ion-Pairs. Both the static density functional calculations and the molecular dynamics simulations demonstrate that the counterion is outside of the coordination sphere of the zirconium at the insertion transition state. In light of the growing evidence to suggest that the insertion potential energy surfaces are very different for ion-pairs and the cationic fragments, the behavior of the anion after the first insertion is an important issue to consider when estimating subsequent insertion barriers. The reactions of a second molecule of ethylene with the Cp_2ZrBu−$MeB(C_6F_5)_3$ ion-pair (structure **4** in Figure 5) was investigated to further study the role of the counterion in subsequent insertions. The first possibility that has already been suggested by the ADF calculations is an associative mechanism where the counterion reestablished coordination with the metal center after insertion had taken place. The potential energy surface for subsequent insertions would be similar to that found for insertion into contact ion-pairs if this mechanism is followed. The second possibility is a dissociative mechanism where the counterion continues to move away from the cationic metal center after insertion. The potential energy surface for the subsequent insertions would be similar to those found for the zirconocene cations if this mechanism is followed.

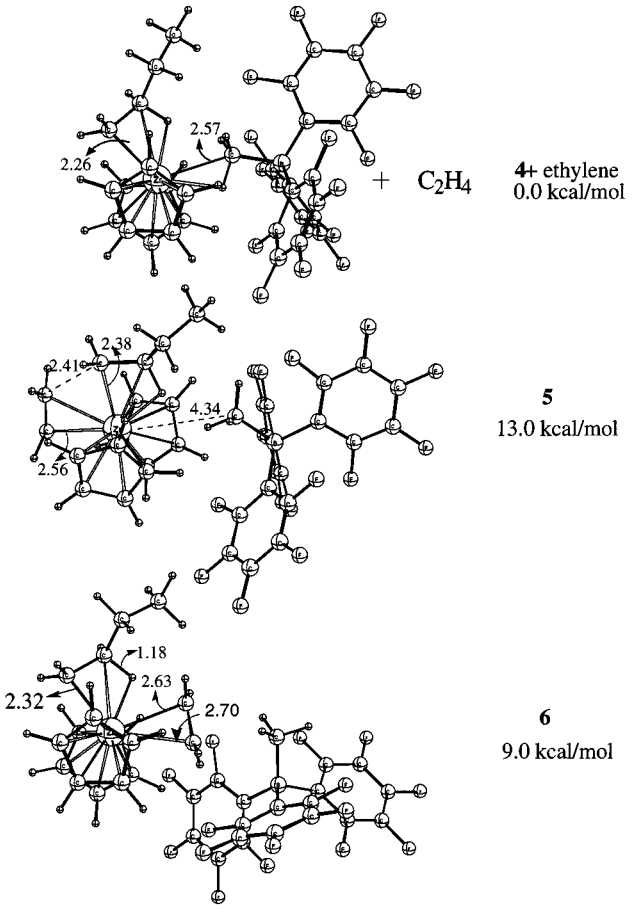

Figure 6. Structure and relative energies of ethylene complexes with the Cp_2ZrEt−$MeB(C_6F_5)_3$ ion-pair.

Two stationary points for the ethylene complexes were found, and their structures and relative energies are shown in Figure 6. One of the complexes (structure **5**) lies 13.0 kcal/mol above the sum of **4** and an ethylene molecule. This ethylene complex can be generated by the approach of the olefin on the side opposite the anion. The midpoint of the olefin is located 2.52 Å from the zirconium, and the anion has left its coordination sphere with a $C_{(methyl)}$−Zr distance of 4.34 Å. There are some changes in the conformation of the butyl chain even though the β-agostic interaction is retained, the most significant being the lengthening of the $C_{(\alpha)}$−Zr bond to 2.38 Å as compared with 2.26 Å in **4**. This long bond distance coupled with the observation that the α carbon is only 2.41 Å from the nearest olefinic carbon suggests that this complex may be, or is very close in structure to, the transition state for the second insertion. More detailed investigations of the potential energy surface around this point by varying the $C_{(\alpha)}$−$C_{(olefin)}$ distance confirm this assignment as the energy is lowered when this distance is shortened or lengthened slightly. This complex provides an estimate for the insertion barrier encountered should the pathway for subsequent insertions follow the associative mechanism that includes the formation of the contact ion-pair after each insertion.

(28) Woo, T. K.; Margl, P. M.; Ziegler, T. *Organometallics* **1997**, *16*, 3454. (b) Margl, P. M.; Lohrenz, J. C. W.; Ziegler, T.; Blöchl, P. *J. Am. Chem. Soc.* **1996**, *118*, 4434.

Table 1. Effect of Solvent Polarity on Ion-Pair Dissociation Energy: Enthalpy Change of $Cp_2ZrBu-C_2H_4-MeB(C_6F_5)_3 \rightarrow Cp_2ZrBu-C_2H_4^+ + MeB(C_6F_5)_3^-$

solvent	epsilon	ΔH (kcal/mol)
gas phase	1.00	49.7
toluene	2.38	16.4
chlorobenzene	5.71	2.6
dichloromethane	9.08	−1.0

The second olefin complex found (structure **6**, Figure 6) can be considered as an intermediate for the dissociative mechanism since the $C_{(methyl)}-Zr$ bond has to break before it can be formed. It is a result of the ethylene molecule approaching the metal center from between the butyl chain and the anion. There is little change in the conformation of the butyl chain; however, the anion has been separated from the metal center with a $C_{(methyl)}-Zr$ distance of 5.58 Å. This structure is similar to the olefin-separated ion-pairs previously studied for methylmetallocene catalysts.[7a] The energy of this complex lies 9.0 kcal/mol above the contact ion-pair **4** and a molecule of ethylene. However, even at this distance, the electrostatic interactions are fairly strong, as indicated by the large positive enthalpy change of 49.7 kcal/mol required to dissociate this ion-pair into its ionic fragments $[Cp_2ZrBu-C_2H_4]^+$ and $[MeB(C_6F_5)_3]^-$. However, it is well known that gas-phase calculations usually overestimate the enthalpy of reactions involving the separation of neutral complexes into its ionic components.[7,8] Therefore, the enthalpy change associated with the dissociation of **6** is calculated in several different solvents to account for solvation effects. The enthalpy change for the various solvents studied are summarized in Table 1. When solvation energies were taken into account, a dramatic decrease in the dissociation energy was observed even in relatively nonpolar solvents such as toluene. As expected, dissociation into the separated ions becomes more and more favorable as the solvent polarity is increased. The free energy change (ΔG) for such a dissociation process would become negative in more polar solvents such as chlorobenzene and dichloromethane when entropic contributions are factored in since the reaction increases the total number of molecules. Therefore, the dissociative insertion mechanism via olefin-separated ion-pairs cannot be ruled out, especially in polar solvents.

IV. Conclusions

The insertion of one molecule of ethylene into the $Cp_2ZrEt-MeB(C_6F_5)_3$ ion-pair was examined by a combination of static density functional methods and first-principles molecular dynamics by the projector-augmented wave method. The most stable conformer of the contact ion-pair can be described as having the anion coordinated to the zirconium on the backside of the ethyl chain and without any agostic interactions. This conformer is 3.2 kcal/mol more stable than the next lowest energy minimum found. This is in contrast to the results obtained from other theoretical studies on metallocene cationic fragments where conformers with β-agostic interactions were found to be important intermediates.[4,25a] The most favorable insertion pathway found was for the ethylene to approach the metal center from the opposite side of where the anion is coordinated. As the ethylene approaches, the ethyl chain rotates toward the anion while at the same time the distance between the zirconium and the methyl group in the anion is lengthened. By the time that coordination of the ethylene actually occurs, this distance had increased to 3.3 Å, basically eliminating the counterion from the coordination sphere of the metal. The insertion process occurs rapidly and without apparent barrier after successful complexation of the ethylene molecule to the metal center. In contrast with previous studies with the metallocene cations, the present investigation suggests that olefin complexation may be the largest barrier to overcome in the insertion into ion-pairs. The kinetic product with the γ-agostic butyl chain was obtained in the dynamics simulations.

The structure of the insertion transition state obtained from both the ADF calculations and the CP-PAW simulations shows that the counterion had been displaced from the coordination sphere of the metal. The behavior of the counterion after the first insertion can have large influences on the mechanism and energy profile of subsequent insertions. Gas-phase ADF calculations indicate that an associative mechanism, where the counterion recombines with the cationic fragment to form a new contact ion-pair, is a possibility. The insertion barriers calculated for the ethyl and butyl contact ion-pairs were found to be 11.6 and 13.0 kcal/mol, respectively. A dissociative mechanism where the counterion continues to separate from the cationic fragment via olefin-separated intermediates was also a possibility when solvation effects were taken into account. The energies required for this process would be the formation of the olefin-separated ion-pair from the contact ion-pair (∼9 kcal/mol), the dissociation into ionic fragments, which is highly dependent on solvent polarity, and finally the insertion barrier of ∼5 to 7 kcal/mol previously obtained for the zirconocene cation.[25a]

Acknowledgment. This investigation was supported by the Natural Science and Engineering Research Council of Canada (NSERC) and by Novacor Research and Technology (NRTC) of Calgary, Alberta, Canada.

Supporting Information Available: Tables of gas-phase energies and Cartesian coordinates of DFT-optimized structures for **1a**−**d**, **2a**−**c**, **3**, **4**, **5**, and **6** as well as the structure of **S1**−**6** from the PAW simulation. This material is available free of charge via the Internet at http://pubs.acs.org.

OM000486S